

Supplementary Material

Single-Step Fabrication of Polymer Nanocomposite Films

*Christoph O. Blattmann and Sotiris E. Pratsinis**

Particle Technology Laboratory ETH Zürich, Sonneggstrasse 3, 8092 Zürich, Switzerland
*pratsinis@ethz.ch

S1. Nanocomposite films with a low PVA solution concentration ($C_p = 1/128$ wt%)

Figure S1 shows SEM cross-section images of a SiO_2 -PVA nanocomposite film prepared in a single-step (Figure 1) using a low PVA concentration ($C_p = 1/128$ wt %) in the sprayed polymer solution and depositing for $t = 4$ min. Its average thickness (~ 370 nm, yellow arrows in Figure S1a) is as expected slightly thinner but similar to that of films prepared for same deposition duration where polymer solutions with higher C_p (1/16 and 1/32 wt %) are used (Figure 2). The planar surface seen in Figures S1a is identical to that obtained with higher C_p (Figure 2). Regardless of the low C_p of the sprayed polymer solution, the SiO_2 nanofiller (bright spots) is homogeneously distributed within the PVA matrix (Figure S1b) also in agreement with what is obtained in films where higher C_p is used (Figure 2).

Such films are expected to exhibit a filler content that is greater than 25 vol% as this is obtained already when more PVA ($C_p = 1/32$ wt %, Figure 2) is added. Such high filler loading with this small nanoparticle size ($d_{\text{SiO}_2} = 20$ nm) is difficult to obtain [1] especially when homogeneity is demanded. The flexibility to add such high filler content significantly enhances the attractiveness of this already rapid and single-step fabrication.

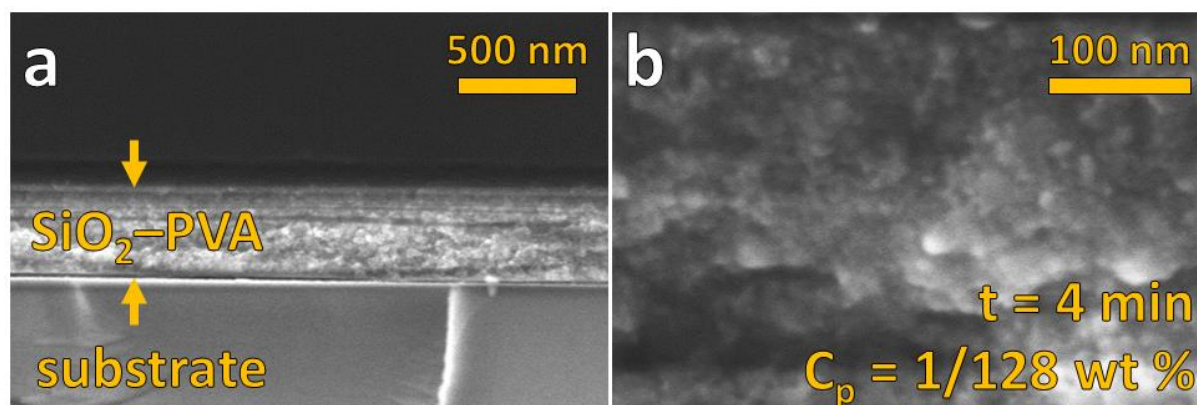


Figure S1. SEM cross-section images of a SiO_2 -PVA nanocomposite film prepared with a polymer solution containing $C_p = 1/128$ wt % PVA and depositing for $t = 4$ min on a glass substrate. Bright spots in **a** and **b** correspond to SiO_2 filler within the PVA matrix (light grey). Yellow arrows in **a** indicate the film thickness.

S2. Pure SiO₂ nanoparticle deposition

High versatility of single-step nanocomposite fabrication enables the preparation of pure nanoparticle films by spraying a polymer-free solution ($C_p = 0$ wt %) during nanoparticle deposition. Figure S2 shows SEM cross-section images of such a film at different magnifications prepared with SiO₂ nanoparticles ($t = 4$ min, $C_f = 0.25$ M). These films exhibit a rougher topography (Figure S2a) due to nanoparticle agglomerates protruding from its surface. Such a protrusion is enlarged in Figure S2c. There one can see the nanoparticulate features covering its surface. Their dimensions are in agreement with the expected nanoparticle size ($d_{\text{SiO}_2} = 20$ nm).

These films exhibit a compact morphology where individual nanoparticles within the bulk film cannot be recognized. This contrasts starkly to the SiO₂-PVA nanocomposites (Figure 2 and Figure S1) where individual nanoparticles are seen throughout the entire film cross-section. The compact film morphology also differs substantially from the highly porous ones obtained during regular flame aerosol deposition [2].

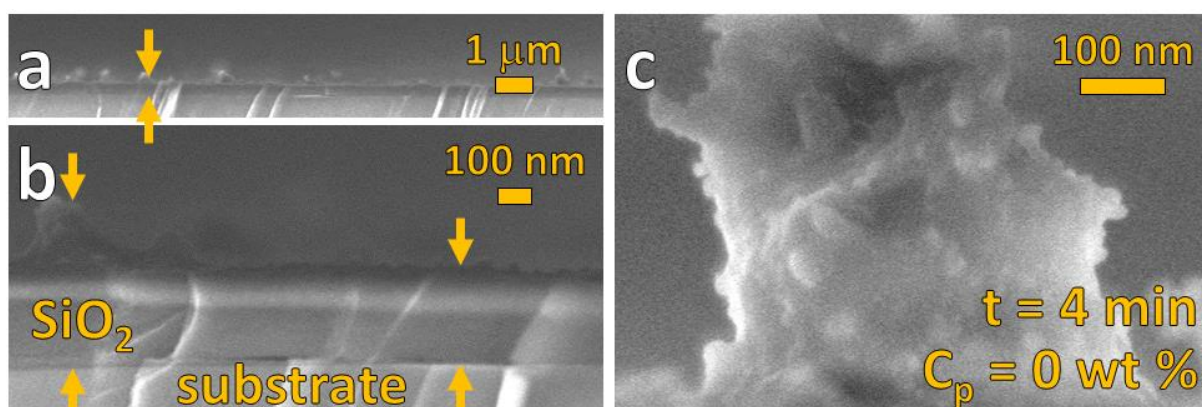


Figure S2. SEM cross-section images of a pure SiO₂ nanoparticle film prepared with a polymer-free PVA solution ($C_p = 0$ wt %) and depositing for $t = 4$ min. The topography is much rougher (a) due to protrusions (c) from its surface. The compact film morphology can be seen in b. The yellow arrows in a and b indicate the film thickness.

S3. Theoretical nanocomposite film thickness

Changing the filler content in SiO₂–PVA nanocomposites by *only* varying the polymer solution concentration C_p (i.e. identical flame synthesis precursor concentration C_f and deposition duration t) leads to a constant total amount of deposited/incorporated nanoparticles (i.e. $m_{\text{SiO}_2} = \text{constant}$) but unavoidably alters the resulting film thickness (higher filler loading for lower C_p of polymer solution).

Figure S3 shows the theoretical PVA nanocomposite thickness as a function of filler content (red line) for a film exhibiting $m_{\text{SiO}_2} = 0.115 \text{ mg}$ of SiO₂ and covering an area of $A_{\text{NC}} = 4 \text{ cm}^2$. This film thickness does not scale linearly with filler content. It changes drastically for <25 vol % nanoparticles. At higher loading this change becomes increasingly smaller until a compact SiO₂ layer is obtained (i.e. 100 vol %).

Experimentally derived values for SiO₂–PVA nanocomposites (circles) prepared with $C_p = 1/8$ and $1/32 \text{ wt } \%$ and depositing for $t = 4 \text{ min}$ (Figure 2c,e) are in good agreement with the theoretical trend. This indicates that the amount of SiO₂ filler depositing on the substrate is independent of added PVA. As a result, once the SiO₂ deposition rate (here: $\sim 7.2 \mu\text{g}\cdot\text{cm}^{-1}\cdot\text{min}^{-1}$) is determined, one is able to quickly predict the filler loading solely from the nanocomposite film thickness and deposition duration t .

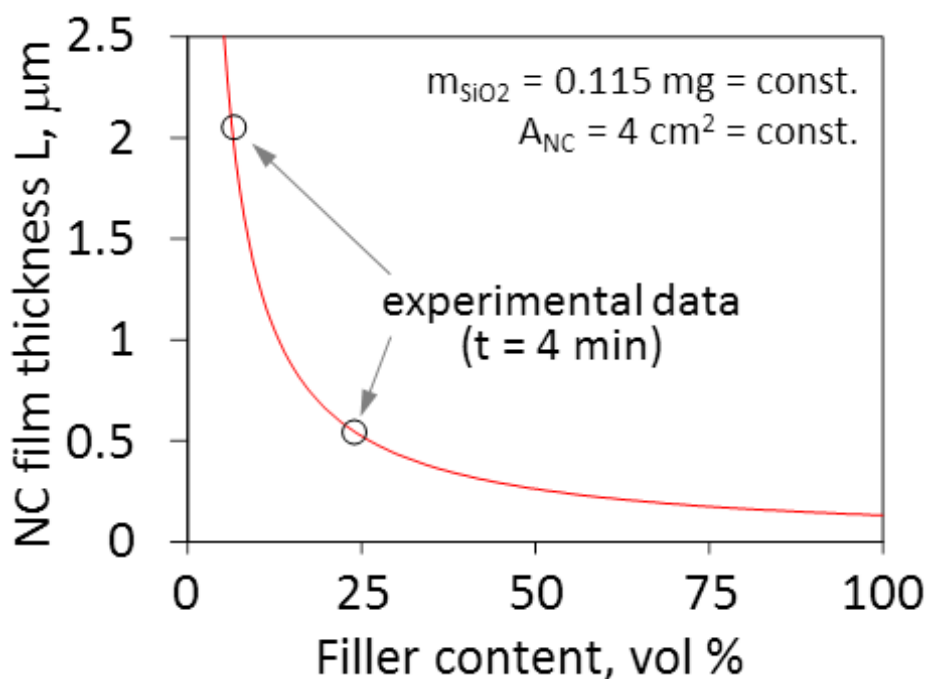


Figure S3. The non-linear correlation of theoretical film thickness (red line) as a function of filler content for PVA nanocomposite films containing identical amount of SiO₂ nanoparticles ($m_{\text{SiO}_2} = 0.115 \text{ mg} = \text{constant}$) and covering the same area ($A_{\text{NC}} = 4 \text{ cm}^2 = \text{constant}$). The thickness changes less at high filler content agreeing well with experimental measurements (circles) shown in Figure 2.

S4. Filler-free polymer deposition

Single-step fabrication of polymer nanocomposites (Figure 1) is capable of achieving agglomerate-free films with extreme variability of filler content. It is easily tuned by (1) increasing polymer solution concentration (C_p), (2) its feed-rate or (3) the rate at which nanoparticles are synthesized. On the one extreme, filler-free polymers can be prepared by either employing a particle-free flame or eliminating the flame altogether. Figures S4 shows SEM cross-section images of pure PVA films prepared on glass substrates with a particle-free flame. The deposition duration t is identical (2 min) for all three images whereas the polymer solution concentration C_p is varied between 1/8 (Figure S4a), 1/16 (Figure S4b) and 1/32 wt % (Figure S4c).

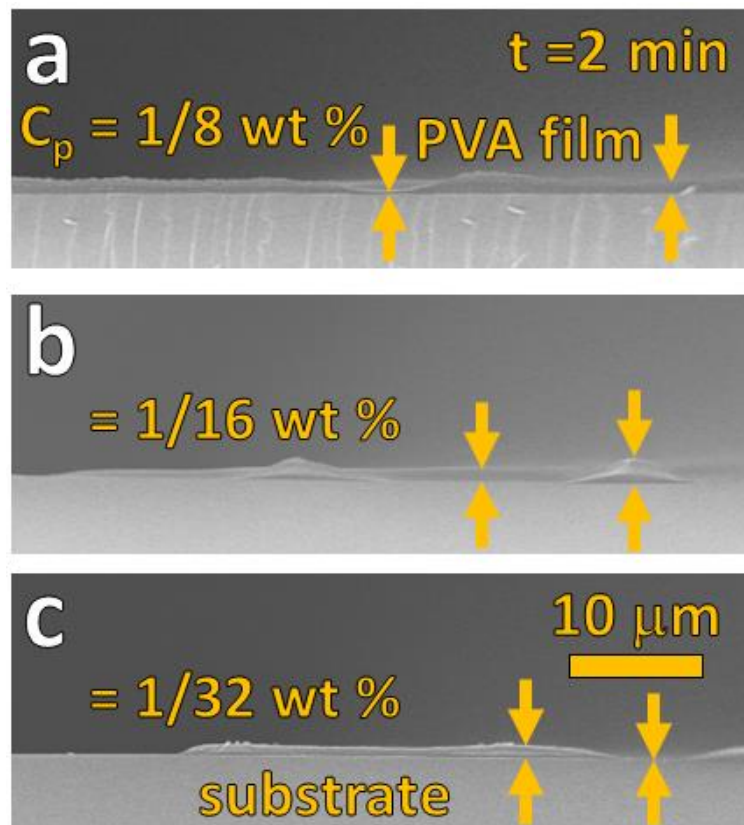


Figure S4. Filler-free PVA films prepared with a polymer solution concentration $C_p = 1/8$ (a), $1/16$ (b) and $1/32$ wt % (c) exhibit an uneven surface topography. The yellow arrows indicate the strong variation in film thickness. The deposition duration ($t = 2$ min) is same for all films. The scale bar shown in c is identical for all images.

In contrast to nanocomposites with filler (Figure 2-4, Figures S1), these exhibit a less planar surface topography for all C_p . In fact, there even are areas where PVA does not cover the substrate. More planar film surface obtained with nanoparticle addition (Figure 2) stems from the surface wetting induced by nanoparticles [3]. Nevertheless, optimization of the fabrication by adjusting the substrate temperature or eliminating the particle-free flame may

improve the film formation for pure polymers [4]. Alternatively, the deposition can be carried out on a vibration-assisted substrate as this has shown efficacy for preparing homogeneous polymer films with and without fillers [5].

S5. References

1. Camenzind, A.; Caseri, W.R.; Pratsinis, S.E. Flame-made nanoparticles for nanocomposites. *Nano Today* **2010**, *5*, 48-65.
2. Mädler, L.; Roessler, A.; Pratsinis, S.E.; Sahm, T.; Gurlo, A.; Barsan, N.; Weimar, U. Direct formation of highly porous gas-sensing films by in-situ thermophoretic deposition of flame-made Pt/SnO₂ nanoparticles. *Sens. Actuator. B-Chem.* **2006**, *114*, 283-295.
3. Cruz, S.; Rocha, L.A.; Viana, J.C. Enhanced printability of thermoplastic polyurethane substrates by silica particles surface interactions. *Appl. Surf. Sci.* **2016**, *360*, 198-206.
4. Felton, L.A. Mechanisms of polymeric film formation. *Int. J. Pharm.* **2013**, *457*, 423-427.
5. Soltani-Kordshuli, F.; Zabihi, F.; Eslamian, M. Graphene-doped PEDOT:PSS nanocomposite thin films fabricated by conventional and substrate vibration-assisted spray coating (svasc). *Eng. Sci. Technol. Int. J.* **2016**, *19*, 1216-1223.